Testing Impedance Eduction Boundary Conditions with Four Wavenumbers per Frequency

André Mateus Netto Spillere*, Lucas Araujo Bonomo† and Júlio Apolinário Cordioli‡
Federal University of Santa Catarina, 88040-900 Florianópolis, Brazil

Edward James Brambley§
University of Warwick, Coventry CV4 7AL, United Kingdom

Impedance eduction of acoustic liners with flow typically calculate different impedances for sound sources upstream and downstream of the liner, despite the physical liner being unchanged. Recent attempts to reduce these differences have considered impedance boundary conditions with additional wavenumber dependent degrees of freedom (for example modelling unsteady momentum transfer between the fluid and the liner). However, any model with an additional degree of freedom at each frequency results in a perfect collapse of upstream and downstream educed impedances, since there are generally only two duct modes per frequency over the liner, one propagating upstream and one downstream. It has therefore been difficult to validate any of these impedance boundary conditions.

Here, a novel experiment is described that is able to investigate four wavenumbers per frequency, each of which are propagating plane wave duct modes, with the same liner and the same flow. By comparing the impedances educed in these four situations, the validity of impedance boundary models may be tested.

I. Introduction

Acoustic liners used in aircraft engines to reduce noise are characterized by their acoustic impedance $Z(\omega, k)$. At an acoustic liner, the acoustic pressure $\mathrm{Re}\big(\tilde{p}\exp\{\mathrm{i}\omega t - \mathrm{i}kx\}\big)$ causes an oscillatory velocity into the liner $\mathrm{Re}\big(\tilde{v}\exp\{\mathrm{i}\omega t - \mathrm{i}kx\}\big)$, with $Z(\omega, k) = \tilde{p}/\tilde{v}$. If $Z(\omega, k)$ is known, it can be used as a boundary condition in models or simulations of aircraft engine noise. Usually, the acoustic liner is considered to be locally reacting, meaning Z is independent of the wavenumber k and depends only on the frequency ω. In such cases, $Z(\omega)$ can be measured using a normal incidence impedance tube. A number of models exist for the impedance $Z(\omega)$ given the design and geometry of the liner [e.g. 1], and agree well with normal incidence impedance tube experimental results.

Experimental measurements of acoustic impedance can also be made at grazing incidence using apparatus such as shown schematically in fig. 1. Loudspeakers excite plane acoustic waves in a duct (below the cuton frequency of higher order duct modes), and microphones record the transmitted and reflected sound from an acoustically lined test region of the duct. From these measurements, and a model of the acoustic propagation within the lined test region, the impedance $Z(\omega)$ can be inferred; this process is referred to as impedance eduction. Without mean flow, good agreement is found between such experimental measurements and normal incidence impedance tube measurements.

Unfortunately, a mean flow across the surface of the acoustic liner significantly modifies the effective impedance seen by acoustics within that mean flow. Until relatively recently, the Ingard–Myers [2, 3] boundary condition was used to model this effect, and results in the boundary condition

$$\frac{\tilde{p}}{\tilde{v}} = Z_{\mathrm{eff}} = \frac{\omega Z}{\omega - U_0 k}, \tag{1}$$

where U_0 is the slipping velocity of the mean flow at the impedance boundary. Even if the liner is locally reacting, so that $Z(\omega)$ is independent of the wavenumber k, the Ingard–Myers boundary condition shows that the effective impedance Z_{eff} seen by the acoustics within the mean flow is no longer locally reacting, but depends on the wavenumber k. In theory, it should still be possible to recovery the impedance Z from the effective impedance Z_{eff}, with measurements from a

*PhD Student, Federal University of Santa Catarina.
†MSc Student, Federal University of Santa Catarina.
‡Associate Professor, Federal University of Santa Catarina.
§Associate Professor, University of Warwick, AIAA senior member.

downstream or upstream source producing the same results. However, experimental tests carried out on different test configurations and using different impedance eduction techniques have consistently showed different results between upstream and downstream sources [e.g. 4–6]. Since the only difference between upstream- and downstream-propagating plane waves is their axial wavenumber k, this is evidence that the k-dependence of the impedance boundary model Z_{eff} being used to educe the impedance is incorrect.

Relatively recently it was shown [7] that the Ingard–Myers boundary condition is illposed and leads to unphysical instability in models and simulations. The illposed behaviour is removed by accounting for a thin mean flow boundary layer within the impedance boundary condition, leading to a significantly more complicated dependence of Z_{eff} on the axial wavenumber k,

$$\frac{\tilde{p}}{\tilde{v}} = Z_{\text{eff}} = \frac{\mathrm{i}\omega Z + \rho_0(\omega - U_0 k)^2 \delta I_0}{\mathrm{i}(\omega - Uk) - \omega Z k^2 \delta I_1 / \big(\rho_0(\omega - U_0 k)\big)}, \tag{2}$$

$$\delta I_0 = \int_0^h 1 - \frac{\big(\omega - U(y)k\big)^2 \rho(y)}{(\omega - U_0 k)^2 \rho_0}\,\mathrm{d}y, \qquad \delta I_1 = \int_0^h 1 - \frac{(\omega - U_0 k)^2 \rho_0}{\big(\omega - U(y)k\big)^2 \rho(y)}\,\mathrm{d}y,$$

where $U(y)$ and $\rho(y)$ are the mean flow velocity and density within the boundary layer, h is the thickness of the boundary layer, and outside the boundary layer $U = U_0$ and $\rho = \rho_0$. Using this boundary model to educe impedance was found to reduce but not eliminate the discrepancy between upstream- and downstream-educed impedances [8].

Further boundary conditions attempt to model the effects of viscosity within the thin boundary layer at the impedance wall [9–12], of which the most notable for its simplicity is that of Aurégan et al. [9]. Correcting the mislabelling of Y and Y_c in that paper, and neglecting temperature variations (as per Renou and Aurégan [4]), this boundary condition in the present notation is

$$\frac{\tilde{p}}{\tilde{v}} = Z_{\text{eff}} = \frac{\omega Z}{\omega - (1 - \beta_\nu) U_0 k}, \qquad \beta_\nu = \frac{1}{U_0} \int_0^h \frac{\mathrm{d}U}{\mathrm{d}y} \exp\big\{ - y\sqrt{\mathrm{i}\omega/\nu} \big\}\,\mathrm{d}y, \tag{3}$$

where ν is the kinematic viscosity and $\mathrm{Re}(\sqrt{\cdots}) > 0$. Renou and Aurégan [4] showed that if the formula for β_ν in (3) is ignored and instead β_ν is best fitted to experimental results, then the upstream and downstream educed impedances can be made to collapse onto a single curve, and moreover that the inferred β_ν performs as expected, with $\beta_\nu \approx 0$ at high frequencies and $\beta_\nu \approx 1$ at low frequencies. (Note that Renou and Aurégan [4] use the notation Z_{eff} for a different quantity to that used here.) Other similar models with extra parameters that could be used to collapse the experimental data include those of Schulz et al. [13] and Aurégan [14], both of which model an axial momentum transfer between the liner and the acoustics. It should, however, be noted that Weng et al. [15] concluded that viscosity is not able to collapse the upstream and downstream educed impedances, while Nark et al. [6] found that small corrections to the mean flow velocity were sufficient to collapse the upstream and downstream educed impedances.

However, if all duct modes but the two plane-wave-like modes are cutoff in the test region, as in all the experimental studies cited here, then there are only two different axial wavenumbers k that occur in the impedance eduction, namely the upstream and downstream plane wave wavenumbers. Therefore, any extra frequency-dependent parameters β which can be best-fitted to the data, such as δI_0 and δI_1, or β_ν, will be enough to collapse the upstream- and downstream-educed impedances. It is therefore hard to test the predictive validity of any of these models. This was noted by Aurégan [14], who wrote "When only two values of the complex wavenumber k are known, they can always be described using two complex numbers such as [Z and β_ν in the notation here]. A true validation of these models can only be achieved when more than two wavenumbers are known. This can be done experimentally or numerically either by determining, at a given configuration, the higher order modes, which are generally strongly attenuated, or by increasing the channel size to have more propagating (or slightly attenuated) modes." Here, we consider a third possibility.

We describe an experiment that allows the investigation of four axial wavenumbers per frequency, with the same acoustic lining and the same flow. The collapse of all four educed impedances is then a test of the validity of any of the above boundary conditions, since best fitting one free parameter would in general be expected to only be able to collapse two of the four impedances.

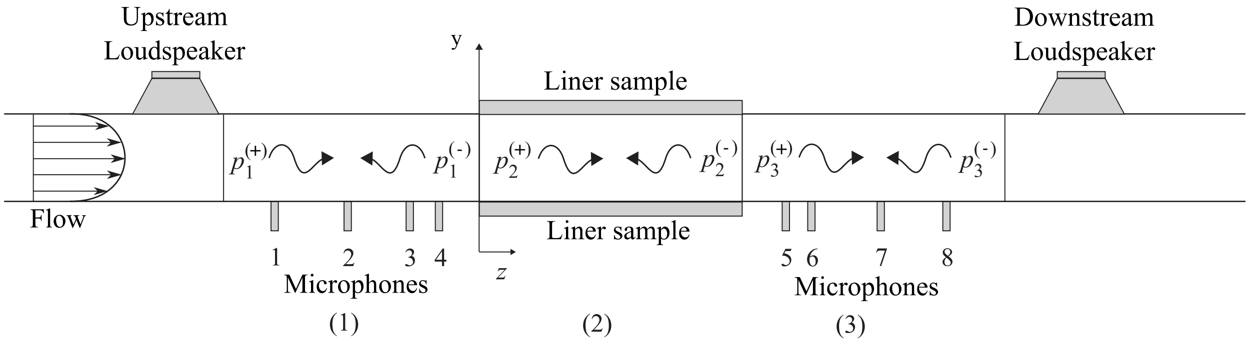

Fig. 1 Schematic of the experiment. A steady flow of velocity $U(y)$ propagates down the rectangular cross-section duct. Loudspeakers are located upstream and downstream of the test section (region 2). The top and bottom walls of the test section may be hard or may be lined with an acoustic impedance Z. Microphones are installed along the walls upstream (region 1) and downstream (region 3) of the test section.

II. Experimental setup

We consider the situation shown schematically in fig. 1, with a rectangular duct containing a steady mean flow. The duct contains a liner test section (region 2), where the top, bottom, or both surfaces can be either lined or unlined (hard-walled). Upstream (region 1) and downstream (region 3) of the test section are wall mounted microphones, and beyond these are two or more wall-mounted loudspeakers. For any given setup of the test section, measurements are made from all microphones of a frequency sweep from the upstream loudspeaker, and from the downstream loudspeaker. The data from the microphones are then analysed to infer the transmitted and reflected acoustic waves, from which the impedance of the liner used in the test section may be educed, as detailed in section III below. The majority of this is standard practice, and the novel innovation here is the lining of either one or both of the walls.

The same experimental rig used for the previous study of impedance boundary conditions [8] is used. The test rig is situated at the Federal University of Santa Catarina (UFSC), Brazil, photographs of which are shown in fig. 2. The cross-section of the duct is 4 cm by 10 cm, for which the no-flow cuton frequency for the first transverse mode is 1700 Hz. Since the microphones are positioned at the half-height of the duct, they are on the nodal line for this first higher order mode, and hence this mode is not captured. The second transverse mode cuts on at 3400 Hz, and so the frequency range tested is from 500 Hz to 2500 Hz in this study. The lined section accommodates liners of length 210 mm, although liner lengths were reduced in some cases up to 115 mm using tape to cover the liner holes in order to reduce attenuation in frequency ranges where the attenuation was too large compared with the background flow noise. The pressure measurements are processed into complex frequency response functions $p^{q}_{\text{exp}}(\omega)$ at each microphone $q = 1, \dots, 8$, giving the amplitude and phase difference of that microphone compared with the microphone closest to the loudspeaker used. The loudspeakers produce a sound pressure level of 130 dB. Results are presented for mean flow Mach numbers of 0.21 and 0.28, calculated by averaging over the duct cross-section. The centre-line Mach number is calculated from a pitot tube and temperature probe measuring centre-line velocity and temperature, and this centre-line Mach number is then converted into a duct-averaged Mach number by multiplying by a pre-calibrated conversion factor; for this particular experiment, a conversion factor of 0.90 was used. The flow is driven by a compressed air reservoir, with a control system regulating the flow to maintain a constant Mach number. The duct upstream and downstream of the test section is treated to have a low reflection coefficient, and the impedance eduction described in §III is designed to take account of, and be relatively robust to, any upstream or downstream reflections.

The two identical liners used were conventional one-degree-of-freedom honeycomb liners supplied by UTC Aerospace Systems (now Collins Aerospace). The liner cavities were 48.6 mm deep, with 1 mm thick facing sheets with 1 mm diameter holes and a 7.4% open area. These parameters were verified experimentally using a normal incidence impedance tube; the liners were found to be identical, apart from a slight variation in the percentage of open area.

Experiments are performed considering three configurations: (i) a lined top wall and a hard bottom wall; (ii) a lined bottom wall and a hard top wall; and (iii) both walls lined. In all cases the same liner is used. The results of the lined/hard and hard/lined cases should be the same, and give an indication of any errors due to asymmetries in the liners, liner holder, or flow. The main purpose of this study is to compare upstream- and downstream-incident sound on a lined/hard and lined/lined test section, which gives four different acoustic wavenumbers for the same liner.

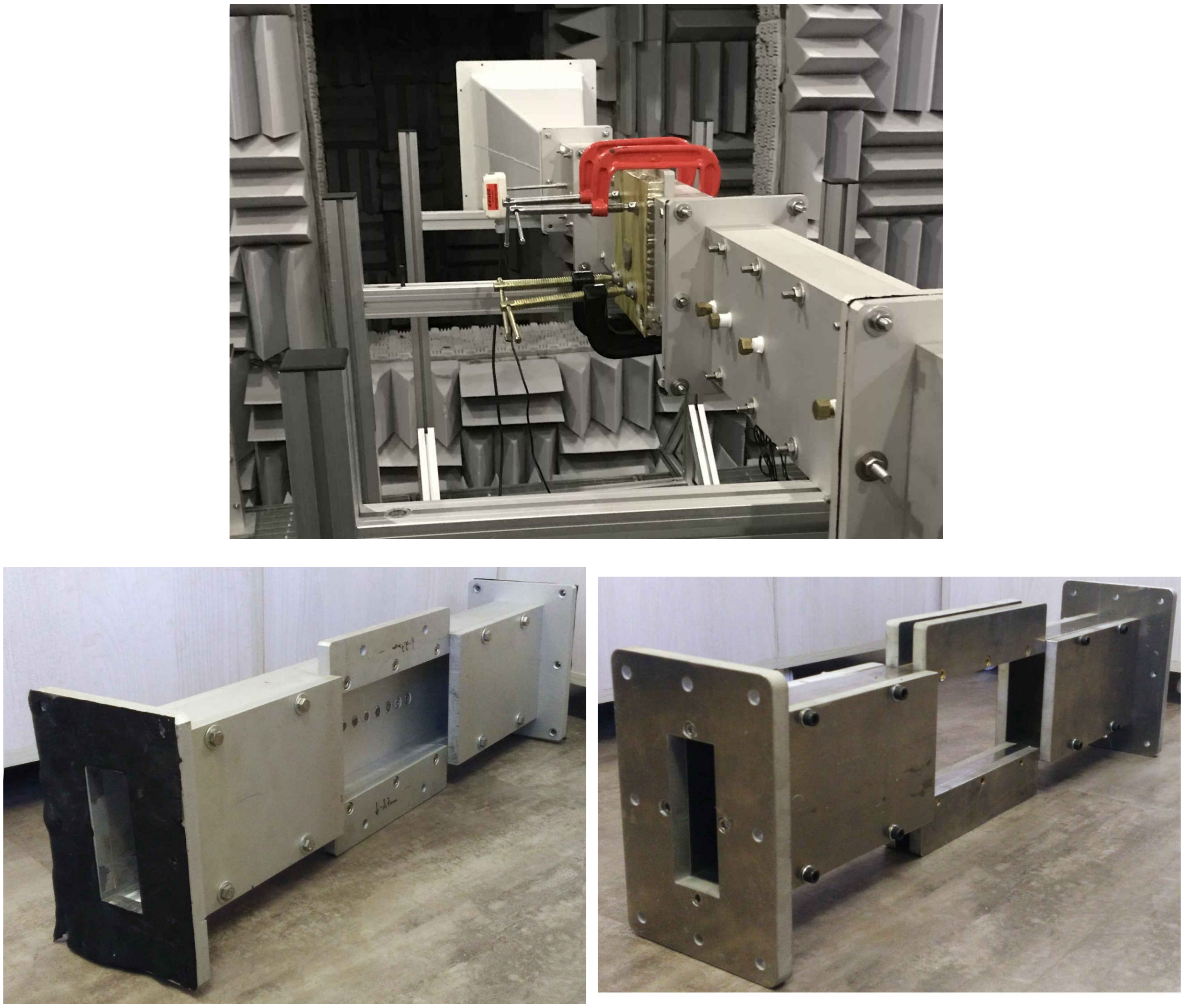

Fig. 2 Photographs of the experimental setup. Top: The impedance eduction duct set up with the the one-sided liner holder [as per 8]. Left: The one-sided liner holder removed from the duct [as per 8]. Right: The two-sided liner holder for the present study. Note that the liners referred to as installed on the "top" and "bottom" surfaces in the text were in practice installed on the left and right of the duct.

III. Impedance Eduction

The same impedance eduction technique is used here as was used by Spillere et al. [8], which makes use of the Mode Matching Method (MMM) of Elnady et al. [16]. In this technique, the acoustics in regions $j = 1$, 2 and 3 (as shown in fig. 1) are decomposed into a sum of duct modes,

$$p_j(x, y, z) = \sum_{n=1}^{N} a_{jn}^{+}\psi_{jn}^{+}(x, y)\mathrm{e}^{-\mathrm{i}k_{jn}^{+}z} + \sum_{n=1}^{N} a_{jn}^{-}\psi_{jn}^{-}(x, y)\mathrm{e}^{-\mathrm{i}k_{jn}^{-}z}, \tag{4}$$

where the first sum is for modes propagating downstream and the second is for modes propagating upstream. For uniform flow, assuming any effects of sheared mean flow are included within the impedance boundary condition, the duct modes are given by

$$\psi(x, y) = \cos(k_x x)\big[A\cos(k_y y) + B\sin(k_y y)\big] \qquad \text{where} \qquad (\omega - U_0 k_z)^2/c_0^2 = k_x^2 + k_y^2 + k_z^2, \tag{5}$$

and c_0 is the speed of sound in the uniform mean flow. The hard wall boundary conditions at the duct sides gives $k_x = n\pi/L_x$ for integer n, where $L_x = 10\,\text{cm}$ is the duct width. The constant A/B and wavenumber k_y are given by

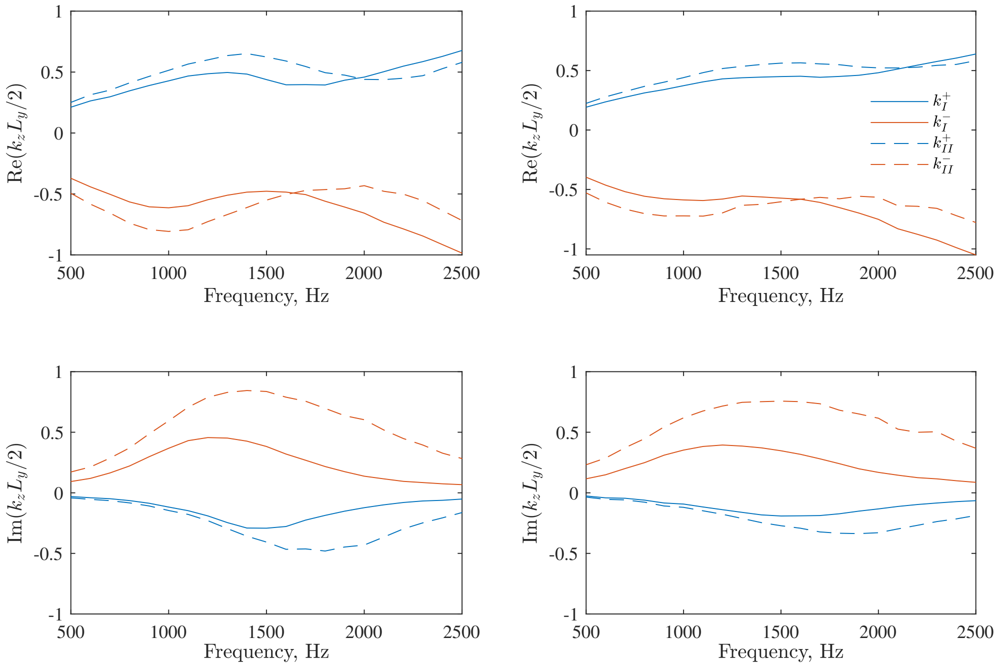

(a) $M = 0.21$ (b) $M = 0.28$

Fig. 3 Educed axial wavenumbers of the most dominant downstream (+) and upstream (−) duct modes in the lined test section with a single lined wall (k_I), as a function of the frequency, for mean-flow Mach numbers (a) $M = 0.21$ and (b) $M = 0.28$. Also shown are the predicted axial wavenumbers with two lined walls (k_{II}). The top plots give the real part of the axial wavenumber, and the bottom plots give the imaginary part of the axial wavenumber. Axial wavenumbers are predicted through the impedance eduction using the Myers boundary condition for liner sample L_{24}**, the impedance of which is plotted in fig. 4.**

satisfying the boundary conditions at the top ($y = L_y/2$) and bottom ($y = -L_y/2$) walls, with $L_y = 4$ cm, giving

$$Z_{\mathrm{eff}} = \frac{\mathrm{i}\rho_0(\omega - U_0 k_z)}{k_y \tan(\eta k_y L_y)} \qquad \text{where} \qquad \begin{cases} \eta = 1, & \text{one lined wall} \\ \eta = 1/2, & \text{two lined walls} \end{cases} \tag{6}$$

The modes of the duct in region 2 therefore depend on the liner impedance Z, whether only one wall ($\eta = 1$) or both walls ($\eta = 2$) are lined, and the boundary condition used to impose the impedance; this includes any free parameters β used in the impedance boundary condition. At the boundaries between the regions 1 and 2, and regions 2 and 3, pressure and axial particle velocity are matched. The microphone measurements from the experiments are decomposed into plane waves, and the plane waves propagating towards the lined section (downstream in region 1 and upstream in region 3) are used to set the plane wave coefficients a_{11}^+ and a_{31}^-. The mode matching then results in a linear system whose solution gives all the coefficients in (4).

Fig. 3 compares the dominant axial wavenumbers $k_z(\omega)$ predicted in the lined test section, using the Myers boundary condition (1). The difference between the axial wavenumbers when only one wall is lined or when both the top and bottom walls are lined is clear, and is especially dramatic for the upstream propagating mode. This demonstrates that the lined/hard and lined/lined test cases really are significantly different, despite using the same impedance linings, frequencies, flow speeds, and other parameters.

Once all the coefficients in (4) are calculated, the pressure $p^q_{\mathrm{MMM}}(Z)$ predicted by the Multi-Modal Method at the location of microphone q may be compared with the actual recorded pressure p^q_{exp}. At each frequency ω, and assuming known values for any free parameters β, the impedance $Z(\omega)$ is educed by minimizing the residual e over all Z, where

$$e(Z) = \sum_{q=1}^{8} \left| \frac{p^q_{\mathrm{exp}} - p^q_{\mathrm{MMM}}(Z)}{p^q_{\mathrm{exp}}} \right|^2 . \tag{7}$$

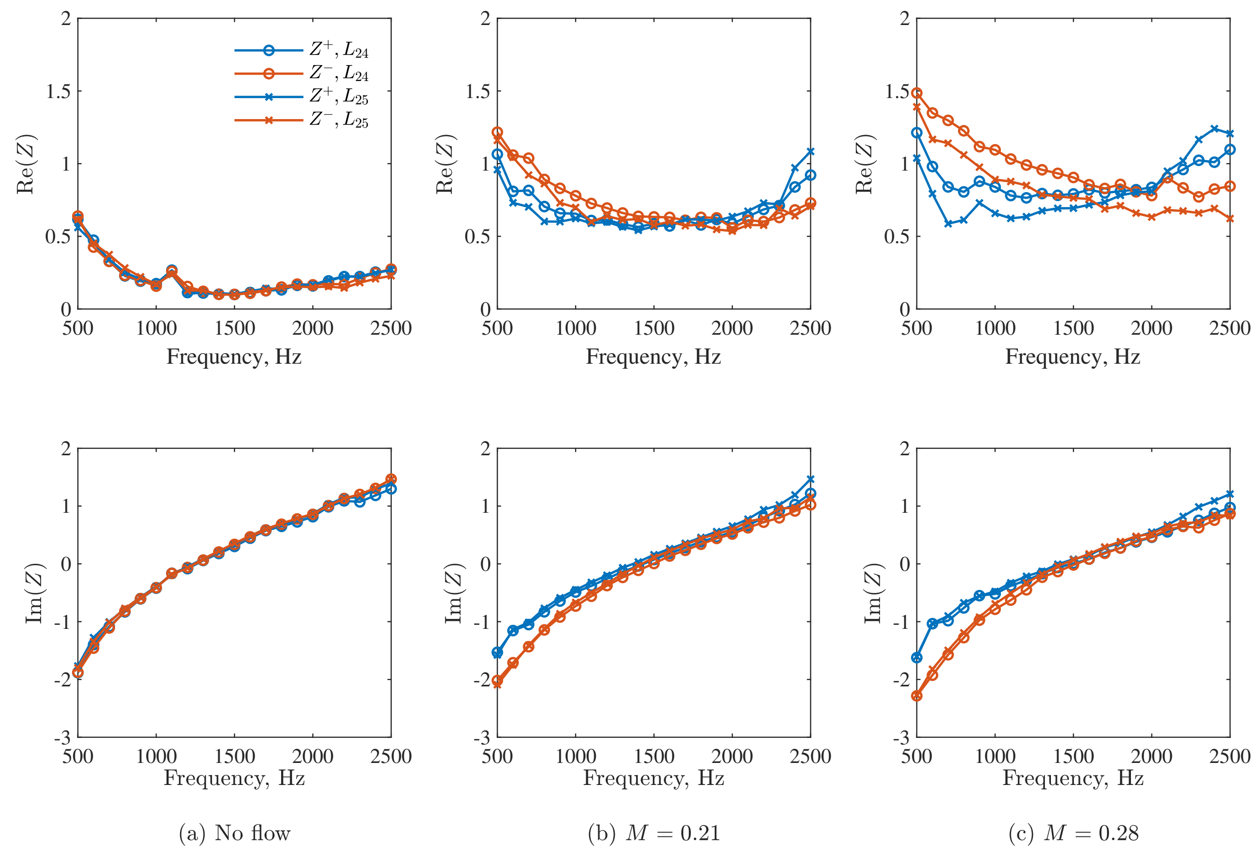

Fig. 4 Educed impedance as a function of frequency, for both upstream (−) and downstream (+) propagation, for the lined/hard (L_{24}) and hard/lined (L_{25}) configurations.

This procedure is performed for the upstream loudspeaker and one wall or both walls lined, and for the downstream loudspeaker with one wall or both walls lined, yielding four different educed impedances $Z(\omega)$.

For each of the lined/hard and lined/lined configurations, using the boundary condition of Aurégan et al. [9] given in (3), the upstream and downstream educed impedances may then be collapsed to the same value by the unique choice of the free parameter $\beta_v(\omega)$, as described by Renou and Aurégan [4, eq. (26)]. Thus, the upstream and downstream lined/hard results lead to a pair $\big(Z(\omega), \beta_v(\omega)\big)$ specifying the impedance boundary condition, and similarly the upstream and downstream lined/lined results lead to a $\big(Z(\omega), \beta_v(\omega)\big)$ pair. A good collapse of these two (Z, β_v) results at each frequency would validate the impedance model being used, which has not been possible with previous studies that only educe two different impedances leading to only one pair (Z, β_v).

IV. Results

Initially, results from using one liner on the bottom of the duct and a rigid wall on the top were compared with using the second liner on the top of the duct and a rigid wall on the bottom. Since the two liners are notionally identical, this comparison would highlight any asymmetries in the liners, the liner holders, or the mean flow. Fig. 4 compares the educed impedance for these two cases. In general, excellent agreement is seen. The small discrepancy in resistance, especially noticeable at $M = 0.28$, may be related to a slight difference in the effective POA of the test samples. The procedure was repeat with interchanged liner and hard wall positions, and the same impedances were obtained, confirming the absence of asymmetries in the test rig.

Fig. 5 shows the educed impedances for lined/hard and lined/lined cases, both upstream and downstream, using the Myers boundary condition. The lack of collapse of the educed impedances shows that the axial wavenumber dependence of the effective impedance $Z_{\text{eff}}(k, \omega)$ is not correct for the Myers boundary condition. This reproduces the known disagreement between impedance educed using upstream and downstream propagation.

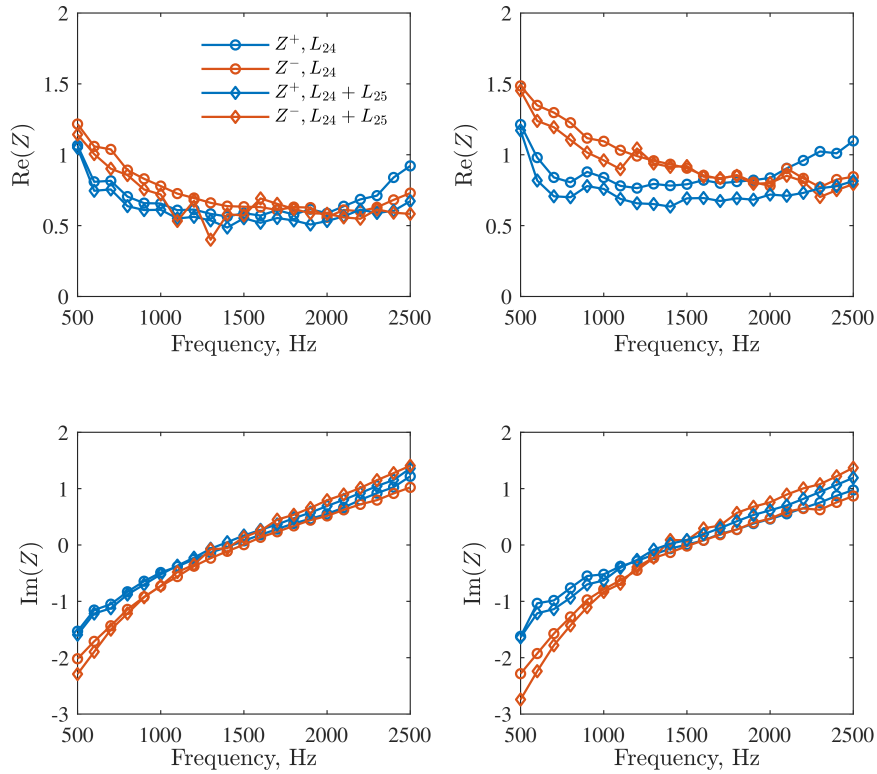

(a) $M = 0.21$ (b) $M = 0.28$

Fig. 5 Educed impedance as a function of frequency, for both upstream (−) and downstream (+) propagation, for the lined/hard (L_{24}) **and lined/lined** ($L_{24} + L_{25}$) **configurations.**

Fig. 6 shows the educed impedances for the two lined/hard and the lined/lined cases using the boundary condition (3) of Renou and Aurégan [4], with the free parameter β_v best fitted to collapse the upstream and downstream educed impedances to the same value. Compared with fig. 5, there is much less variability in the educed impedances in the top two plots in fig. 6, as is to be expected from best fitting an extra free parameter. The impedances educed for the lined/hard configuration (labelled L_{24} and L_{25}) and the lined/lined configuration (labelled $L_{24} + L_{25}$) are very close, although for the lined/lined case the educed resistance is systematically underestimated at high frequencies, and the educed reactance is systematically overestimated for frequencies above the first resonance and systematically underestimated for frequencies below the first resonance, all at both tested Mach numbers. For the best-fitted free parameter $\beta_v(\omega)$, plotted in the lower two plots of fig. 6, however, there is a significant disparity between each of the configurations above 1500 Hz. The imaginary part of β_v is close to zero, and the real part is close to 0.5 at low frequencies (although theoretically we should have $\beta_v(\omega) \to 1$ as $\omega \to 0$). However, at higher frequencies $\beta_v \approx 0$ for the lined/lined configuration, while β_v becomes significantly negative for the lined/hard configurations. It would certainly appear, therefore, that the educed value of β_v depends on whether one or both sides of the duct were lined, and therefore a single (Z, β) pair is not sufficient to collapse the results of all four wavenumbers.

Another way to verify the educed impedances and their predictive capacity, following Renou and Aurégan [4], is by means of the plane-wave scattering matrix,

$$\begin{bmatrix} a_{31}^+ \\ a_{11}^- \end{bmatrix} = \begin{bmatrix} T^+ & R^- \\ R^+ & T^- \end{bmatrix} \begin{bmatrix} a_{11}^+ \\ a_{31}^- \end{bmatrix}, \tag{8}$$

Fig. 7 (reproduces the results of Renou and Aurégan [4, fig. 9]) shows the experimental and predicted coefficients of the scattering matrix for the lined/hard configuration. Predicted coefficients using the upstream educed impedance, and the downstream educed impedance, are both plotted. In the absence of flow, excellent agreement is found with both educed impedances. On the other hand, in the presence of flow, none of the educed impedances is able to correctly

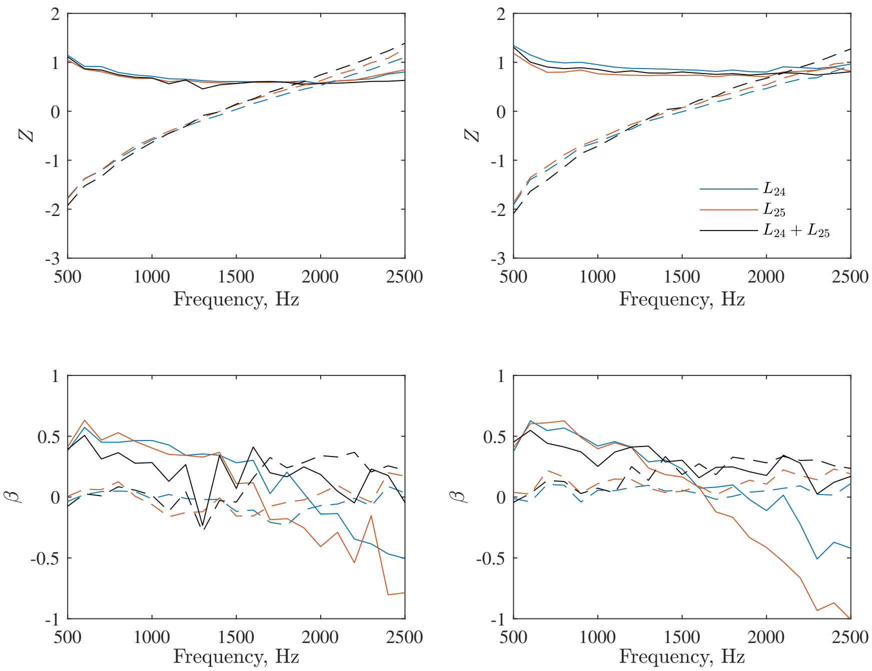

(a) $M = 0.21$ (b) $M = 0.28$

Fig. 6 Educed impedance and the related β_v parameter which collapse the upstream and downstream educed impedances to the same value, using the effective impedance given in equation (3). Solid and dashed lines correspond to real and imaginary parts, respectively.

predict both upstream and downstream coefficients, again demonstrating the inadequacy of the Myers Z_{eff} boundary condition. By using a collapsed impedance with β_v best-fitted, both predicted T^+ and T^- can be made to agree well with experiments, as can be seen in fig. 8. However, fig. 9 shows that the educed β_v model from the lined/hard configuration fails to provide a good prediction in the lined/lined configuration. In particular, the upstream-propagating transmission coefficient T^- is poorly predicted away from low frequencies, and this is true at both Mach numbers considered. This is further evidence that the educed value of β_v is specific to the configuration being investigated, and is not an intrinsic property of either the mean flow or the liner itself.

V. Discussion and Future Work

In this work, for a given impedance lining, average flow Mach number M, and frequency ω, four different axial wavenumbers are tested: upstream and downstream propagating plane waves, in each of a lined/hard and lined/lined configuration. A correct impedance boundary condition $Z_{\text{eff}}(Z, \beta, k)$ should be accurate for each of these four axial wavenumbers, with *the same value of Z and free parameters β for each wavenumber*. The Myers boundary condition has no free parameters, and is known to need different values of Z to correctly predict the propagation of upstream and downstream plane-wave modes. This may be corrected by using the impedance boundary condition of Aurégan et al. [9] if only two axial wavenumbers are used, by suitable choice of the free parameter $\beta_v(\omega)$ at each frequency. In this work, we are unable to find an impedance Z and free parameter β_v that accurately reproduce the experimental results obtained in both our lined/hard and lined/lined configurations. In particular, fig. 6 shows that the value of β_v calculated from our results is specific to the configuration (lined/hard vs lined/lined), while fig. 9 shows that using the (Z, β_v) pair found from the lined/hard configuration does not reproduce the upstream transmission coefficient we observe for the lined/lined configuration; upstream being the situation where the two configurations give most different axial wavenumbers, as shown in fig. 3. Our results therefore suggest that the boundary condition of Aurégan et al. [9] does not have good predictive power beyond the specific configuration used to calculate the impedance and β_v.

One obvious opportunity to extend this work would be to understand and correct for the small disparity between liner samples L_{24} and L_{25} shown in fig. 4. It is unlikely this small disparity between liner samples affects the behaviour

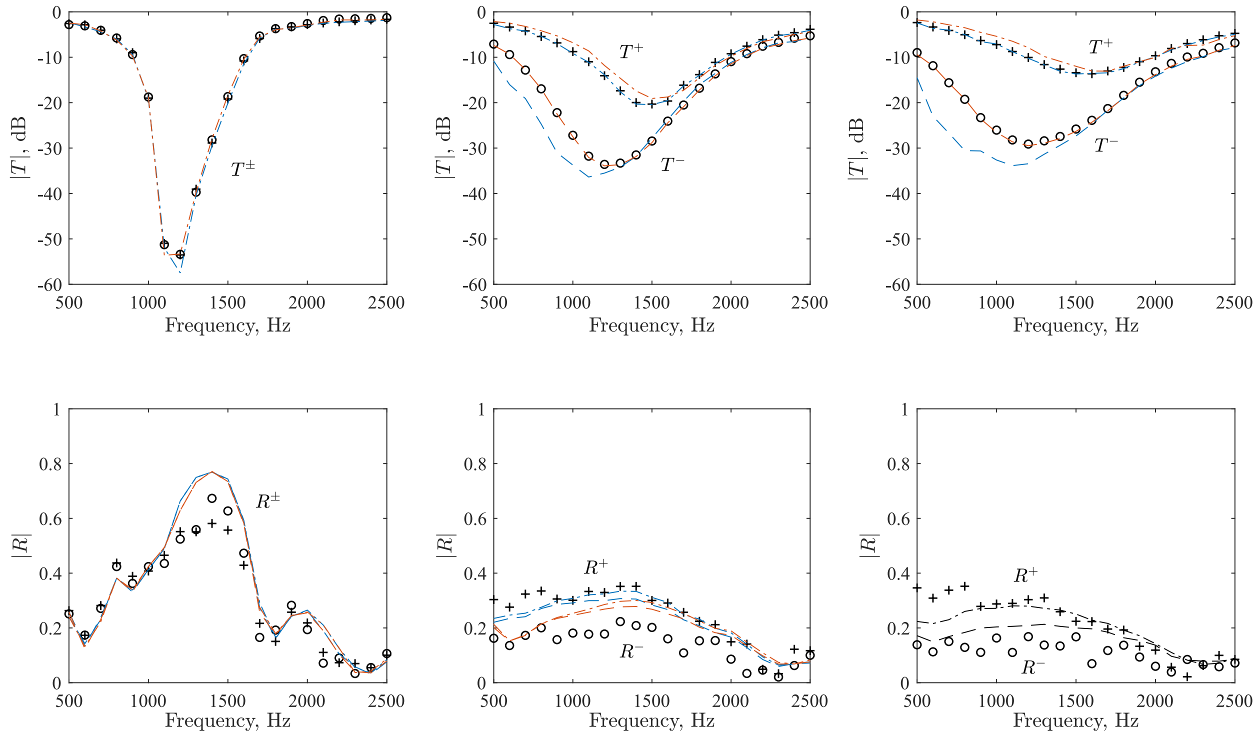

(a) No flow (b) $M = 0.21$ (c) $M = 0.28$

Fig. 7 Experimental scattering coefficients (points) for the lined/hard configuration, and the predicted scattering coefficients using the upstream and downstream educed impedances using the Myers boundary condition (blue and red lines, respectively). Note that a shorter liner of length 115 mm **was used for only the upstream-propagating (**T^- **and** R^-**) results at** $M = 0.28$**, meaning the absolute magnitude of these coefficients at** $M = 0.28$ **is not directly comparable with the other results in this figure.**

seen subsequently, since the disparity in fig. 4 is most significant at $M = 0.28$ and almost negligible at $M = 0.21$, while we subsequently see an equal effect at both Mach numbers.

One possible future extension of this work would be to best fit frequency independent parameters, such as the shear layer velocity profile $U(y)$ involved in the formula for $\beta_v(\omega)$ in (3), rather than treating $\beta_v(\omega)$ as a free parameter to be independently calculated for each frequency ω; this would be expected to give worse agreement with experiments compared with the present study. It would however enable comparison with other boundary conditions, such as that of Ref. 7 given in (2), or more complicated boundary conditions such as that of Khamis and Brambley [12, equ. (54)], that do not provide a single frequency-dependent parameter to be fitted.

Another future extension would be to investigate how well the educed impedance and free parameters from one situation predict the behaviour of liners in other situations. Ultimately, liners are a tool for reducing aeroengine noise, and so educed impedances should be relevant outside the apparatus used to educe the impedance. For example, are educed impedance parameters from narrow rectangular-duct laboratory tests a useful predictive tool for the behaviour of the same liners in large cylindrical ducts more typical of aeroengine installations, or are boundary-layer dependent parameters such as $\beta_v(\omega)$ specific to the laboratory test rig? Moreover, are impedance parameters educed from plane wave propagation a useful predictive tool for higher order modes, such as the spinning modes more typical of fan noise?

Acknowledgments

The authors are grateful to Jose Alonso from UTC Aerospace Systems (now Collins Aerospace) for supplying the liner samples used in this study. AMNS, LAB and JAC gratefully acknowledge funding from CNPq (National Council for Scientific and Technological Development) and FINEP (Funding Authority for Studies and Projects). EJB gratefully acknowledges funding from a Royal Society University Research Fellowships (UF150695).

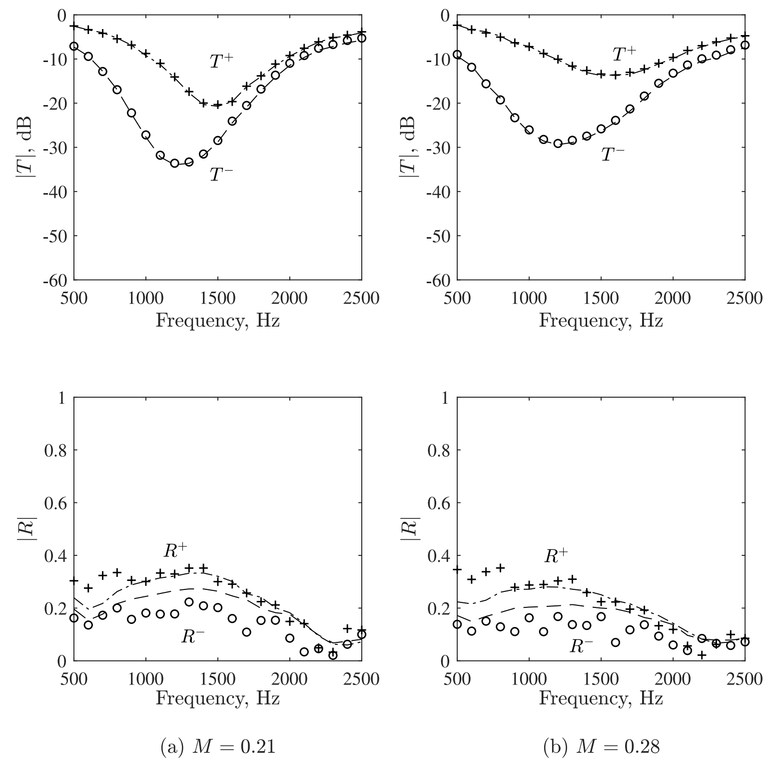

Fig. 8 Experimental scattering coefficients (points) for the lined/hard configuration, and the predicted scattering coefficients (lines) using the collapsed Z and β_v educed from the lined/hard configuration.

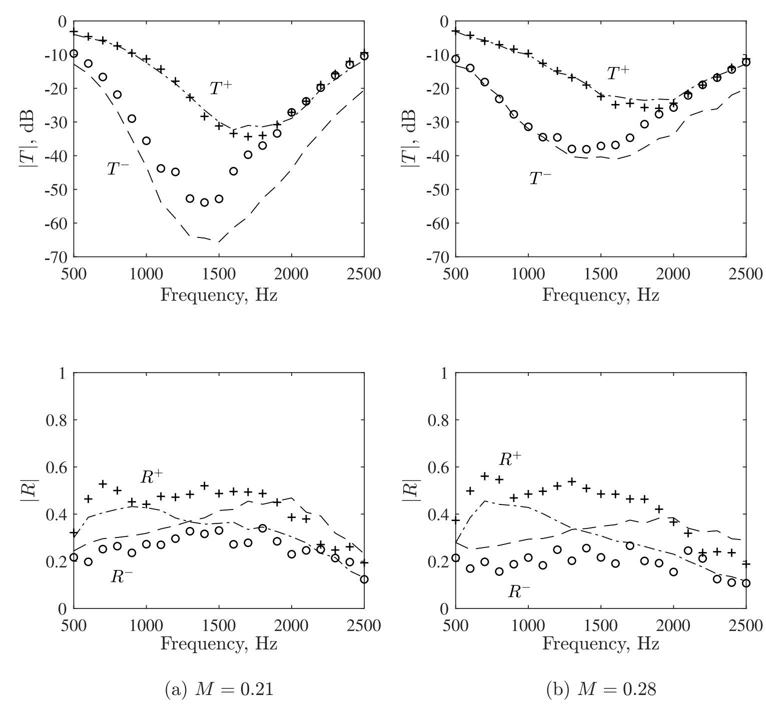

Fig. 9 Experimental scattering coefficients (points) for the lined/lined configuration, and the predicted scattering coefficients (lines) using the collapsed Z and β_v educed from the lined/hard configuration.

References

[1] Rienstra, S. W., “Impedance Models in Time Domain, including the Extended Helmholtz Resonator Model,” AIAA paper 2006-2686, 2006. doi:10.2514/6.2006-2686.

[2] Ingard, U., “Influence of Fluid Motion Past a Plane Boundary on Sound Reflection, Absorption, and Transmission,” *J. Acoust. Soc. Am.*, Vol. 31, 1959, pp. 1035–1036. doi:10.1121/1.1907805.

[3] Myers, M. K., “On the Acoustic Boundary Condition in the Presence of Flow,” *J. Sound Vib.*, Vol. 71, 1980, pp. 429–434. doi:10.1016/0022-460X(80)90424-1.

[4] Renou, Y., and Aurégan, Y., “Failure of the Ingard–Myers Boundary Condition for a Lined Duct: An Experimental Investigation,” *J. Acoust. Soc. Am.*, Vol. 130, 2011, pp. 52–60. doi:10.1121/1.3586789.

[5] Bodén, H., Zhou, L., Cordioli, J. A., Medeiros, A. A., and Spillere, A. M. N., “On the Effect of Flow Direction on Impedance Eduction Results,” AIAA paper 2016-2727, 2016. doi:10.2514/6.2016-2727.

[6] Nark, D. M., Jones, M. G., and Piot, E., “Assessment of Axial Wave Number and Mean Flow Uncertainty on Acoustic Liner Impedance Eduction,” AIAA paper 2018-3444, 2018. doi:10.2514/6.2018-3444.

[7] Brambley, E. J., “Fundamental Problems with the Model of Uniform Flow over Acoustic Linings,” *J. Sound Vib.*, Vol. 322, 2009, pp. 1026–1037. doi:10.1016/j.jsv.2008.11.021.

[8] Spillere, A. M. N., Cordioli, J. A., and Bodén, H., “On the Effect of Boundary Conditions on Impedance Eduction Results,” AIAA paper 2017-3185, 2017. doi:10.2514/6.2017-3185.

[9] Aurégan, Y., Starobinski, R., and Pagneux, V., “Influence of Grazing Flow and Dissipation Effects on the Acoustic Boundary Conditions at a Lined Wall,” *J. Acoust. Soc. Am.*, Vol. 109, 2001, pp. 59–64. doi:10.1121/1.1331678.

[10] Brambley, E. J., “Acoustic Implications of a Thin Viscous Boundary Layer over a Compliant Surface or Permeable Liner,” *J. Fluid Mech.*, Vol. 678, 2011, pp. 348–378. doi:10.1017/jfm.2011.116.

[11] Khamis, D., and Brambley, E. J., “Viscous Effects on the Acoustics and Stability of a Shear Layer over an Impedance Wall,” *J. Fluid Mech.*, Vol. 810, 2017, pp. 489–534. doi:10.1017/jfm.2016.737.

[12] Khamis, D., and Brambley, E. J., “Acoustics in a two-deck viscothermal boundary layer over an impedance surface,” *AIAA J.*, Vol. 55, No. 10, 2017, pp. 3328–3345. doi:10.2514/1.J055598.

[13] Schulz, A., Weng, C., Bake, F., Enghardt, L., and Ronneberger, D., “Modeling of Liner Impedance with Grazing Shear Flow using a New Momentum Transfer Boundary Condition,” AIAA paper 2017-3377, 2017. doi:10.2514/6.2017-3377.

[14] Aurégan, Y., “On the use of a Stress–Impedance Model to describe Sound Propagation in a Lined Duct with Grazing Flow,” *J. Acoust. Soc. Am.*, Vol. 143, No. 5, 2018, pp. 2975–2979. doi:10.1121/1.5037585.

[15] Weng, C., Schulz, A., Ronneberger, D., Enghardt, L., and Bake, F., “Flow and Viscous Effects on Impedance Eduction,” *AIAA J.*, Vol. 56, No. 3, 2017, pp. 1118–1132. doi:10.2514/1.J055838.

[16] Elnady, T., Bodén, H., and Elhadidi, B., “Validation of an Inverse Semi-Analytical Technique to Educe Liner Impedance,” *AIAA J.*, Vol. 47, No. 2, 2009, pp. 2836–2844. doi:10.2514/1.41647.